Experimental and Numerical Characterization of the Flow Around The Mars 2020 Rover

R. Bardera[1], S. Sor[2] and A. Garcia-Magariño[3]
Instituto Nacional de Técnica Aeroespacial (INTA). Torrejón de Ardoz (Madrid). Spain, 28850

and

J. Gómez-Elvira [4], M. Marin [5], S. Navarro [6], J. Torres [7], and S. Carretero [8]
Centro de Astrobiología, INTA-CSIC (CAB), Torrejón de Ardoz (Madrid). Spain, 28850

The investigation of the environmental factors in Mars atmosphere is one of the issues of the NASA's Mars Exploration Program about the potential for life on Mars. The future Mars 2020 rover will transport the Mars Environmental Dynamics Analyzer (MEDA) dedicated to obtain meteorological data, as well as other objectives, about wind speed and direction. High quality of wind data are required to build mathematical models of the Mars climate, therefore, powerful techniques are necessary to eliminate flow perturbations produced by the rover presence. The aim of this paper is the characterization of the flow around the Mars 2020 rover, providing a deep insight into the environmental interaction of the Mars wind with the rover. A comparative study between numerical simulations versus wind tunnel experimental results is conducted trying to investigate the influence of the rover on the flow measured by the MEDA wind sensors. This study is addressed to perform an assessment of the reliability of numerical methods in the prediction of this kind of flow in Martian conditions, evaluating its capability to be used in the future to correct wind data coming from the Mars 2020 rover mission. The advancements in the numerical methods as compared with experimental results

[1] PhD Aerospace Engineer,, Experimental Aerodynamics, barderar@inta.es.
[2] PhD Aerospace Engineer,, Experimental Aerodynamics, sors@inta.es.
[3] PhD Aerospace Engineer,, Experimental Aerodynamics, garciamga@inta.es.
[4] PhD Aerospace Engineer, Advanced Instrumentation, gomezej@inta.es.
[5] Telecomunication Engineer, Advanced Instrumentation, mmarin@cab.inta-csic.es.
[6] Industrial, Advanced Instrumentation, navarrols@cab.inta-csic.es.
[7] PhD Aerospace Engineer, Advanced Instrumentation, torresrj@inta.es.
[8] Industrial Engineer , Advanced Instrumentation, scarretero@cab.inta-csic.es

Published by the American Institute of Aeronautics and Astronautics, Inc., with permission. Complete Citation: Bardera, R., Sor, S., Garcia-Magarino, A., Gomez-Elvira, J., Marin, M., Navarro, S., ... & Carretero, S. (2018). Experimental and numerical characterization of the flow around the Mars 2020 rover. Journal of Spacecraft and Rockets, 55(5), 1136-1143. https://doi.org/10.2514/1.A34217

implies an advancement on the calibration methods in the space wind sensor instrumentation carried in the Mars 2020 rover.

Nomenclature

α_{CFD} = numerical simulation pitch angle

α_{PIV} = experimentally-measured pitch angle

β = yaw angle

CAD = Computer Aided Design

CCD = Charge Coupled Device

CFD = Computational Fluid Dynamics

CPU = Central Processing Unit

ε_α = error in pitch angle measurement

ε_V = velocity error function

FFT = Fast Fourier Transform

FoV = field of view

fs = full scale

L = characteristic length

L_{fs} = full scale length

L_m = model length

λ_L = length scale ratio

λ_ν = kinematic viscosity ratio

λ_V = velocity scale ratio

MEDA = Mars Enviromental Dynamic Analyzer

MMRGT = Multi-Mission Radioisotope Thermoelectric Generator

MSL = Mars Science Laboratory

ms = model scale

μ = dynamic viscosity

Published by the American Institute of Aeronautics and Astronautics, Inc., with permission. Complete Citation: Bardera, R., Sor, S., Garcia-Magarino, A., Gomez-Elvira, J., Marin, M., Navarro, S., ... & Carretero, S. (2018). Experimental and numerical characterization of the flow around the Mars 2020 rover. Journal of Spacecraft and Rockets, 55(5), 1136-1143. https://doi.org/10.2514/1.A34217

Nx = mesh dimension in X direction

Ny = mesh dimension in Y direction

Nz = mesh dimension in Z direction

ν = kinematic viscosity

ν_{fs} = full scale kinematic viscosity

ν_{ms} = model scale kinematic viscosity

P = pressure

PIV = Particle Image Velocimetry

R_{CO2} = gas constant of CO_2

Re = Reynolds number

Re_{fs} = full scale Reynolds number

Re_{ms} = model scale Reynolds number

RSM = Remote Sensing Mast

ρ = density

S = characteristic temperature

T = temperature

T_0 = reference temperature

V = characteristic velocity

V_{CFD} = numerical simulation velocity magnitude

V_{PIV} = experimentally-measured velocity magnitude

V_m = model velocity

V_{fs} = full scale velocity

Vx = wind speed in X direction

Vy = wind speed in Y direction

Vz = wind speed in Z direction

V_∞ = freestream air velocity

Published by the American Institute of Aeronautics and Astronautics, Inc., with permission. Complete Citation: Bardera, R., Sor, S., Garcia-Magarino, A., Gomez-Elvira, J., Marin, M., Navarro, S., ... & Carretero, S. (2018). Experimental and numerical characterization of the flow around the Mars 2020 rover. Journal of Spacecraft and Rockets, 55(5), 1136-1143. https://doi.org/10.2514/1.A34217

I. Introduction

The Mars 2020 rover mission is a part of NASA's Mars Exploration Program designed as a long-term effort for the exploration of Mars. The mission would also provide a way to demonstrate novel technologies addressed to the future human expeditions to Mars.

The investigation of the environmental factors will provide a better understanding of the meteorological processes of the Mars atmosphere. The Mars 2020 rover will host the Mars Environmental Dynamics Analyzer (MEDA), which is the contribution of Spain to the program and that will be dedicated to investigate environmental factors at the Martian surface during the Mars 2020 rover mission. MEDA sensors will provide both ambient and ground temperatures measurements, wind speed and its direction, pressure, relative humidity, ultraviolet radiation, and the size and shape of dust.

MEDA includes a new design of the wind REMS sensor [1, 2] embarked on the Mars Science Laboratory (MSL) Curiosity rover which is based on hot film anemometry [3]. This technology was successfully demonstrated during the Viking mission [4-6].

Two wind sensors booms are located around the Remote Sensing Mast (RSM) and oriented 120 degrees from each other. Sensors are capable of measuring wind speed up to 70 m/s and they are located on the rover mast and affected by the rover's presence. A correction of the wind data is necessary in order to obtain the correct measurements avoiding the flow perturbations produced by the rover [7].

In the past, in previous Mars missions such as the Viking Mars Lander, the influence of the wind field in the vicinity of the lander was investigated by wind tunnel testing a 0.45-scale model and performing flow-field measurements by hot film anemometry [7]. More recently, the Curiosity rover's influence on the REMS wind sensors booms was assessed by numerical simulations performed by Centro de Astrobiología (CAB) [2].

In this paper, the characterization of the flow near the rover is experimentally and numerically investigated in order to evaluate the flow perturbation produced by the presence of the rover. Novel technologies were involved in this investigation: rapid prototyping of the models by additive manufacturing, Particle Image Velocimetry (PIV) for nonintrusive whole velocity field measurements used in wind tunnel tests experiments and numerical simulations

Published by the American Institute of Aeronautics and Astronautics, Inc., with permission. Complete Citation: Bardera, R., Sor, S., Garcia-Magarino, A., Gomez-Elvira, J., Marin, M., Navarro, S., ... & Carretero, S. (2018). Experimental and numerical characterization of the flow around the Mars 2020 rover. Journal of Spacecraft and Rockets, 55(5), 1136-1143. https://doi.org/10.2514/1.A34217

carried-out by Computational Fluid Dynamics (CFD) codes. Finally, a comparative analysis is established between numerical methods (CFD) and experimental techniques in order to validate the effectiveness of numerical methods to correctly predict the flow around the Mars 2020 rover vehicle, and specifically in the velocity and direction of the flow as seen by the MEDA wind sensors, so that Mars wind measurements could be corrected in the future.

II. The Mars 2020 rover

The Mars 2020 rover is a nuclear-powered rover dedicated to the Martian surface exploration that transports a set of scientific instruments to investigate Mars. The rover is basically composed of a central body with rectangular section supported by six wheels, the vertical mast that supports a remote vision camera and MEDA environmental instruments, an articulated robotic arm and the Multi-Mission Radioisotope Thermoelectric Generator (MMRGT) that converts heat from the natural radioactive plutonium into electrical power for engineering systems and science payload of the rover [8]. MMRGT is a cylindrical box connected to heat dissipation fins and two heat exchanger plates [9].

Figure 1 shows the external configuration of the Mars 2020 rover vehicle where main dimensions are detailed in centimeters. A typical length of the rover has been considered as L = 1.70 m.

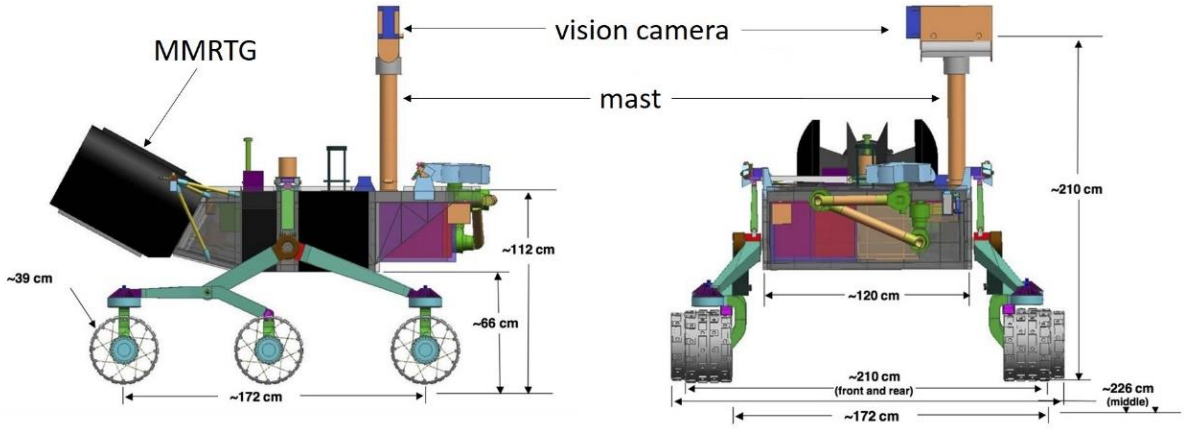

Figure 1. Sketch of Mars 2020 rover .

III. Mars Atmosphere Flow Conditions

The Martian atmosphere is mainly composed of CO_2 with a typical surface pressure of 700 Pa [10] and a variable surface temperature over range from 145 to 245 K [11]. Table 1 shows the main Mars atmospheric parameters

Published by the American Institute of Aeronautics and Astronautics, Inc., with permission. Complete Citation: Bardera, R., Sor, S., Garcia-Magarino, A., Gomez-Elvira, J., Marin, M., Navarro, S., ... & Carretero, S. (2018). Experimental and numerical characterization of the flow around the Mars 2020 rover. Journal of Spacecraft and Rockets, 55(5), 1136-1143. https://doi.org/10.2514/1.A34217

indicating its values. The atmospheric density (ρ) was calculated considering the perfect gases law where the gas constant of CO_2 is R_{CO2} = 188.918 J/kg·K. Dynamic viscosity (μ) was computed following the Sutherland law [12]. Finally, kinematic viscosity (ν) is given as the dynamic viscosity to density ratio. The Reynolds number (*Re*) is a dimensionless parameter that represents the inertial forces ($\sim\rho V^2 L$) to viscous forces ($\sim\mu V/L^2$) ratio and indicates the flow is laminar or turbulent. Reynolds number is a fundamental parameter for a flow simulation that verifies the dynamic similarity. In this work, the flow at maximum Reynolds number (2.4×10^5) is studied corresponding to a Mars flow velocity of V = 40 m/s.

Table 1. Mars atmosphere flow conditions

parameter	expression	units	min value	max value
pressure	P	Pa	700	700
temperature	T	K	145	245
density	$\rho = \frac{P}{R_{CO2}T}$	kg/m^3	2.555×10^{-2}	1.512×10^{-2}
dynamic viscosity (*)	$\mu = \mu_0\left(\frac{T}{T_0}\right)^{3/2}\left(\frac{T_0+S}{T+S}\right)$	N·s/m^2	7.153×10^{-6}	1.235×10^{-5}
kinematic viscosity	$\nu = \frac{\mu}{\rho}$	m^2/s	2.799×10^{-4}	8.163×10^{-4}
Reynolds number	$Re = \frac{\rho VL}{\mu}$	--------	2.4×10^5	8.3×10^4

(*) T_0 = 273 K and S = 222 K (Ref. [12])

IV. Wind Tunnel Experimental Setup

The wind tunnel experiments were conducted in a low speed wind tunnel at INTA (Spain). The wind tunnel is a closed-circuit wind tunnel type with an open test section of 2 × 3 m^2 and a maximum airspeed of 60 m/s. Wind tunnel freestream turbulence intensity is lower than 0.5%. The wind tunnel has a platform that simulates a flat planetary surface. A 1/10th scaled model of the Martian rover was built in plastic material by additive manufacturing techniques as shown in Fig. 2. The two booms containing the MEDA wind speed sensors are located at half of the mast height.

Published by the American Institute of Aeronautics and Astronautics, Inc., with permission. Complete Citation: Bardera, R., Sor, S., Garcia-Magarino, A., Gomez-Elvira, J., Marin, M., Navarro, S., ... & Carretero, S. (2018). Experimental and numerical characterization of the flow around the Mars 2020 rover. Journal of Spacecraft and Rockets, 55(5), 1136-1143. https://doi.org/10.2514/1.A34217

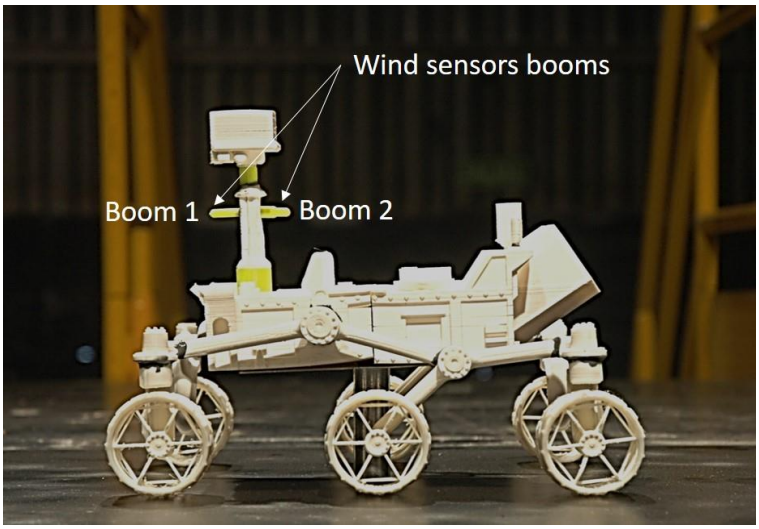

Figure 2. Sketch of Mars 2020 rover

Validity of wind tunnel experiments is based on similarity laws between the full scale (*fs*) and model scale (*ms*). Geometric similarity requires that all dimensions of the model and full scale rover have the same length scale ratio as given by the following expression,

$$\lambda_L = \frac{L_m}{L_{fs}} \qquad (1)$$

where L_m and L_{fs} represent the model and the full scale lengths, respectively. The length scale ratio was selected to be 1/10 in order to avoid flow blockage effects in wind tunnel flow [13].

Kinematic similarity requires that the model and prototype have the same velocity scale ratio λ_V at all points as given by,

$$\lambda_V = \frac{V_m}{V_{fs}} \qquad (2)$$

where V_m and V_{fs} are the model and the full scale flow velocities, respectively.

On the other hand, dynamic similarity requires the same Reynolds number for model and full scale,

Published by the American Institute of Aeronautics and Astronautics, Inc., with permission. Complete Citation: Bardera, R., Sor, S., Garcia-Magarino, A., Gomez-Elvira, J., Marin, M., Navarro, S., ... & Carretero, S. (2018). Experimental and numerical characterization of the flow around the Mars 2020 rover. Journal of Spacecraft and Rockets, 55(5), 1136-1143. https://doi.org/10.2514/1.A34217

$$Re_{ms} = Re_{fs} \qquad (3)$$

Looking at the Mars rover design, aerodynamically it can be considered as a bluff body, so most probably the airflow characteristics around it are relatively insensitive to Re number if it is above a critical Reynold number. However, in this case, due to the differences on the air density and viscosity between Earth and Mars, the same Re number can be attained. Reynolds number is related to kinematic viscosity by the following expression,

$$Re = \frac{VL}{\nu} \qquad (4)$$

Therefore, a relation between length, velocity and viscosity scales is found as follows,

$$\lambda_\nu = \lambda_V \lambda_L \qquad (5)$$

where λ_ν is the kinematic viscosity ratio given by,

$$\lambda_\nu = \frac{\nu_{ms}}{\nu_{fs}} \qquad (6)$$

The kinematic viscosity ratio only depends on the fluid properties corresponding to the wind tunnel rover model (ν_{ms}) and the full scale rover inside the Mars atmosphere (ν_{fs}), so that length and velocity scales must be adapted according to expression (5) to get the same Reynolds number as predicted by the dynamic Reynolds similarity, after equation (3). Kinematic viscosity scale is approximately 0.05 and length ratio was selected to be 0.1, hence velocity scale can be estimated as 0.5, according to expression (5). Therefore, the adequate wind tunnel freestream velocity is approximately 20 m/s, assuming air in standard pressure and temperature conditions.

Published by the American Institute of Aeronautics and Astronautics, Inc., with permission. Complete Citation: Bardera, R., Sor, S., Garcia-Magarino, A., Gomez-Elvira, J., Marin, M., Navarro, S., ... & Carretero, S. (2018). Experimental and numerical characterization of the flow around the Mars 2020 rover. Journal of Spacecraft and Rockets, 55(5), 1136-1143. https://doi.org/10.2514/1.A34217

The wind tunnel experiments were carried out for a free stream velocity of 20 m/s and averaged values of environmental variables during the tests were 944.3 Pa of barometric pressure and 17 ºC of temperature giving a Reynolds number of 2.2×10^5. Different yaw angles of wind incidence were tested in order to study the influence of the rover model on the speed and direction of the wind in the near flow field velocity.

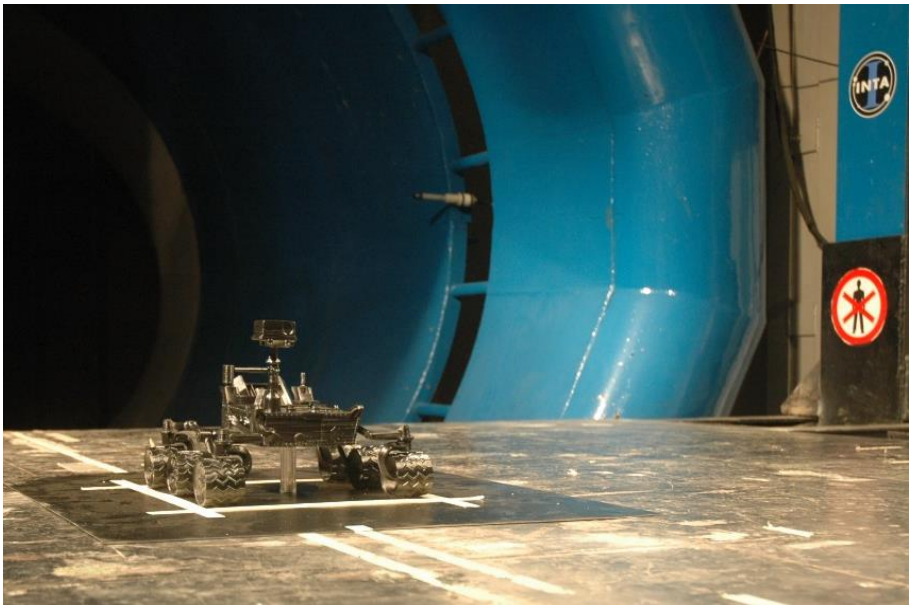

Figure 3. Model of the Martian rover inside wind tunnel test section.

Figure 3 shows the Mars2020 rover model inside the wind tunnel test section. The model was painted flat black in order to avoid laser reflections during the wind tunnel tests campaign.

A. Flow visualization

The flow around the rover model was visualized by injecting smoke. The smoke was produced by an Aerolab smoke generator system that uses white mineral oil as the smoke fluid. Fig. 4 shows the deflection of the streamlines when the smoke jet was steered to the wind sensor booms, thus the angularity of the flow can be clearly observed by the pitch angle denoted as α. Downstream of the mast, a detached turbulent flow can be observed inside the wake.

Published by the American Institute of Aeronautics and Astronautics, Inc., with permission. Complete Citation: Bardera, R., Sor, S., Garcia-Magarino, A., Gomez-Elvira, J., Marin, M., Navarro, S., ... & Carretero, S. (2018). Experimental and numerical characterization of the flow around the Mars 2020 rover. Journal of Spacecraft and Rockets, 55(5), 1136-1143. https://doi.org/10.2514/1.A34217

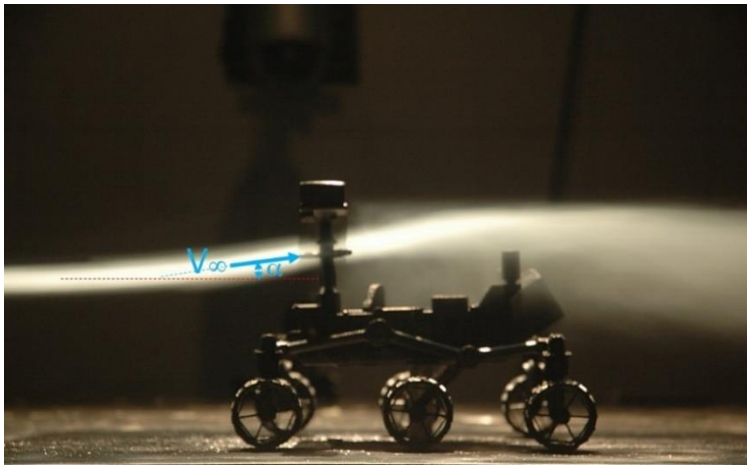

Figure 4. Flow visualization around the Mars 2020 rover.

B. Particle Image Velocimetry measurements

The airflow around the model was experimentally investigated by means of Particle Image Velocimetry (PIV). PIV is a quantitative flow visualization technique used to obtain instantaneous flow field velocity measurements [14-16].

The flow was seeded with olive oil tracer particles (1μm in diameter) produced by an aerosol generator based on Laskin nozzles [17, 18]. Two Nd:YAG (Neodymium: Yttrium Aluminium Garnet) lasers illuminated the flow by delivering the maximum energy output of 190 mJ per pulse. The pulse separation time was 50 μs and the pulses duration was 10 ns so the particle images were sharp and clear on the pictures.

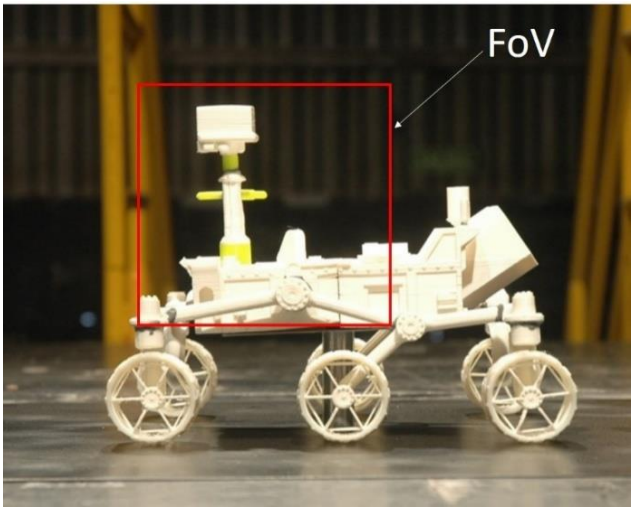

Figure 5. Particle Image Velocimetry Field of View.

The flow field containing tracer particles was illuminated by the laser sheet and recorded by one CCD (Charged Coupled Device) camera with a resolution of 2048×2048 pixels, and equipped with an ED AF Nikkor 80-200mm camera lens. A synchronizer controlled the camera and the time interval between laser pulses. The camera Field of View (FoV) was 270×270 mm^2 (see Fig. 5) and the data rate acquisition of PIV images was 10 Hz.

A cross-correlation analysis implemented via a 2D Fast Fourier Transform (FFT) calculates the averaged displacement of the particles contained within regions of the image known as interrogation windows [19]. Image processing was performed using interrogation windows of 32×32 pixels with a 50% window overlap following the Nyquist sampling criteria. The correlation peak was located by fitting a Gaussian curve with subpixel accuracy. Post processing analysis was executed by detection of vector holes caused by spurious vectors and filling these holes by a local mean filter size of 3×3.

A complete set of PIV images was analysed giving as a result the averaged field over 200 instantaneous maps. After post processing is completed, the mean flow velocity field is obtained and the streamlines are overlapped over the velocity maps.

V. CFD Code

CFD simulations have been used in the frame of the Mars Science Laboratory (MSL) project in the study on wind interactions with the MMRTG [9] and also for thermal plume effects [20] but not for simulations of the flow field around the whole rover.The CFD simulations software used was FloEFD 10 by MENTOR. With this software the external boundary domain and initial condition was set to recreate the same test atmospheric conditions of the wind tunnel tests. The simulations were generated with laminar and turbulent flow features activated. The simulations were also modelled with conduction in solids and free forced convection feature included. FloEFD solves the Navier Stokes equations to predict turbulent flows when the Favre-averaged Navier Stokes equations are used. To close this system of equations, FloEFD uses transport equations for the turbulent kinetic energy and its dissipation rate. The mesh grid was modelled using FloEFD with 2.7 million total cells including solid, fluid and partial cells, which were manually refined in the test area of interest resulting in a locally rectangular mesh for solving the governing equations on it. The 3D model is a simplified version of the NASA rover and the area of interest is the effect of the local perturbation

Published by the American Institute of Aeronautics and Astronautics, Inc., with permission. Complete Citation: Bardera, R., Sor, S., Garcia-Magarino, A., Gomez-Elvira, J., Marin, M., Navarro, S., ... & Carretero, S. (2018). Experimental and numerical characterization of the flow around the Mars 2020 rover. Journal of Spacecraft and Rockets, 55(5), 1136-1143. https://doi.org/10.2514/1.A34217

around the rover mast where the two wind sensors were designed and manufactured by the MEDA team are located. This solid model is identical to the test item tested in INTA facilities in order to compare the error in the CFD simulations to the experimental tests conducted at INTA wind tunnel facilities and evaluate its behaviour for more complex models.

A 1:10 scale model of this rover has been used for the validation of the CFD simulations. Figure 6 shows the CAD model of the 1:10 scale rover. The wind direction and speeds simulated were: $\alpha = 0°$, $0° \leq \beta \leq 330°$ in increments of 30°, and V_{CFD} = 10 and 20 m/s.

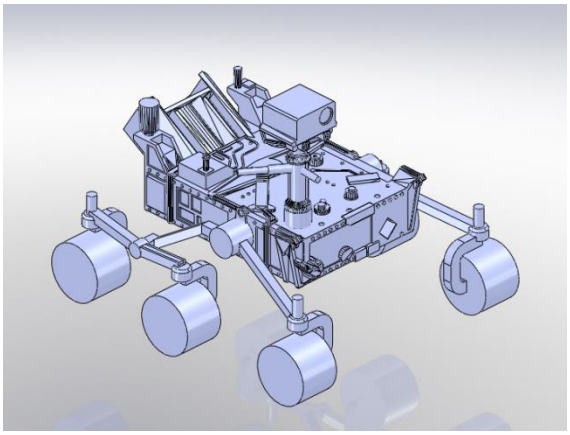

Figure 6. CAD model of the 1:10 scale rover.

A. General Settings and Mesh Size

The fluid computational domain size set for the simulations is 80×78×40 cm^3. A faithful reproduction of the rover geometry was achieved using a fine mesh. The basic mesh dimensions Nx=142, Ny=143, Nz=73 create an initial mesh in the domain of 5 mm mesh size. In addition, six local meshes were used to refine the solid cells in the rover: "wheels and legs left", "wheels and legs right", "mast and camera", "deck", "WS1" and "WS2". The resulting Cartesian mesh consists of 2.7 million cells, which include 1.6 million fluid cells, 800,000 solid cells and 300,000 partial cells. Figures 7 and 8 correspond to Rover solid cells and Fluid cells around the rover, respectively.

The general settings for the simulations are set as follows: pressure of 1 atm., temperature of 288.15 K, Fluid Air and Analysis Type "External". Wind speed and direction are set in the velocity parameters box using the three components of wind speed Vx, Vy, Vz.

Published by the American Institute of Aeronautics and Astronautics, Inc., with permission. Complete Citation: Bardera, R., Sor, S., Garcia-Magarino, A., Gomez-Elvira, J., Marin, M., Navarro, S., ... & Carretero, S. (2018). Experimental and numerical characterization of the flow around the Mars 2020 rover. Journal of Spacecraft and Rockets, 55(5), 1136-1143. https://doi.org/10.2514/1.A34217

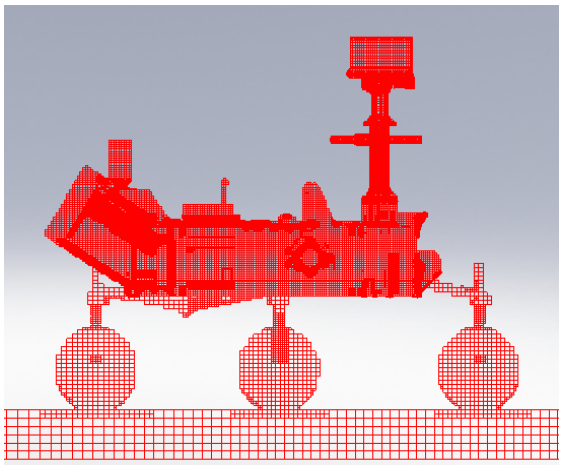

Figure 7. Rover solid cells.

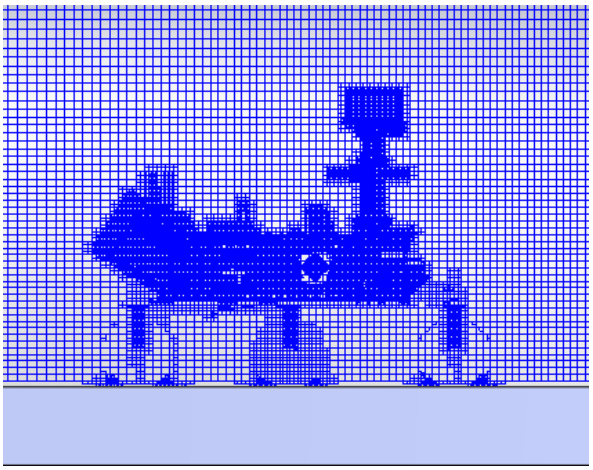

Figure 8. Fluid cells around the rover.

CPU time of computation varied from 6 hours to 10 hours depending on the wind speed and direction.

VI. Results

Results obtained by both, experimental (PIV) and numerical (CFD) techniques are presented as velocity maps in order to provide a more clear visualization of the differences. A comparative analysis is performed by velocity magnitude and direction maps for the more representative flow directions (β = 0, 90, 180 and 270º). Axes of the Mars rover and the flow incidence angle are indicated in Fig. 9.

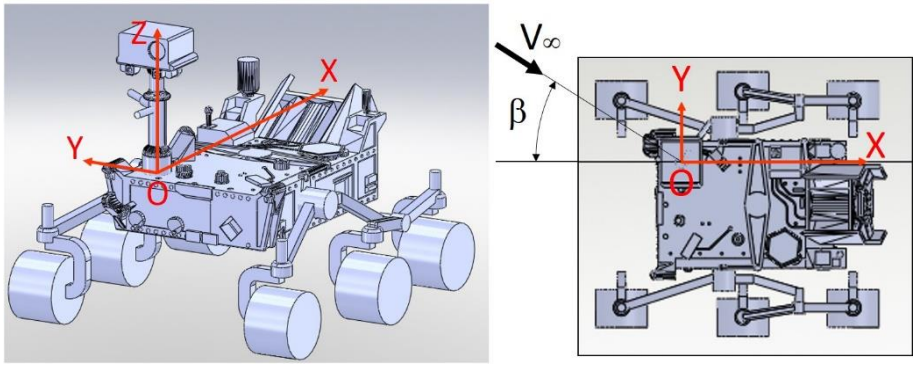

Figure 9. Axis of the Mars 2020 rover (right: top view).

A. Flow field velocity maps

Figure 10 shows the flow field velocity maps obtained by CFD and PIV. Streamlines and vectors overlapped on the maps indicate the flow direction. Color scale legend represents the local velocity magnitude. The flow structure is very similar in both cases. Upstream, the streamlines are slightly curved ($\alpha = 5^{o}$) by the presence of the rover vehicle modifying the velocity received by the sensor booms, as previously demonstrated by the flow visualization. Downstream of the mast, the flow is separated as typically corresponds to the wake of bluff bodies .

Published by the American Institute of Aeronautics and Astronautics, Inc., with permission. Complete Citation: Bardera, R., Sor, S., Garcia-Magarino, A., Gomez-Elvira, J., Marin, M., Navarro, S., ... & Carretero, S. (2018). Experimental and numerical characterization of the flow around the Mars 2020 rover. Journal of Spacecraft and Rockets, 55(5), 1136-1143. https://doi.org/10.2514/1.A34217

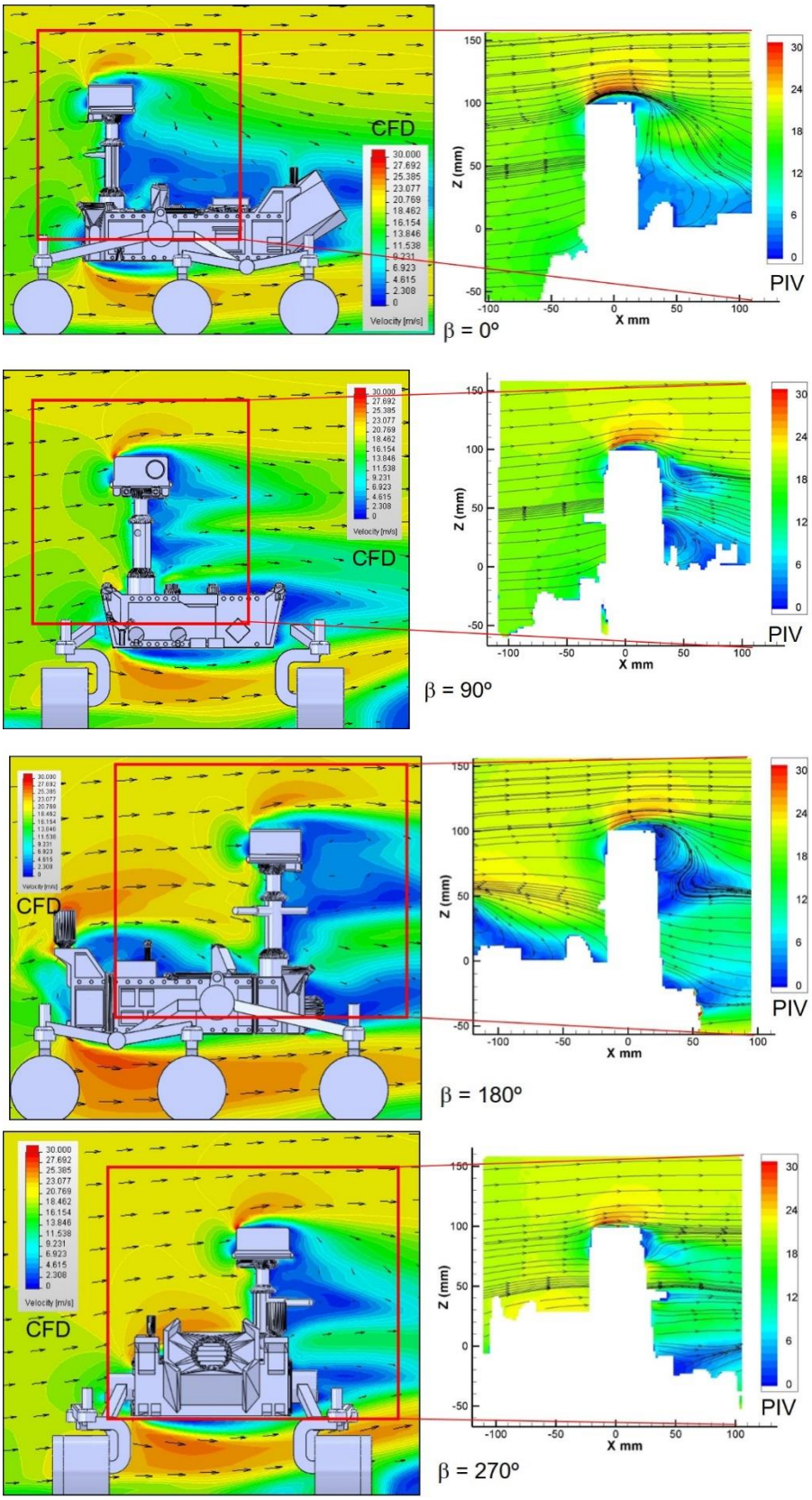

Figure 10. Flow velocity around the Mars 2020 rover.

Published by the American Institute of Aeronautics and Astronautics, Inc., with permission. Complete Citation: Bardera, R., Sor, S., Garcia-Magarino, A., Gomez-Elvira, J., Marin, M., Navarro, S., ... & Carretero, S. (2018). Experimental and numerical characterization of the flow around the Mars 2020 rover. Journal of Spacecraft and Rockets, 55(5), 1136-1143. https://doi.org/10.2514/1.A34217

B. Velocity differences

Differences in velocity magnitude plotted in Fig. 11 are evaluated as an error function $\varepsilon_V(\%)$ defined by the following expression,

$$\varepsilon_V(\%) = \frac{V_{CFD} - V_{PIV}}{V_\infty} \times 100 \qquad (7)$$

where V_{CFD} is the velocity magnitude as calculated by numerical simulation (CFD), V_{PIV} is the velocity magnitude experimentally determined by the PIV technique and V_∞ is the freestream velocity. The color scale represents the percentage of difference in velocity magnitude as determined by both, CFD and PIV. Maps of Fig. 11 are indicating a very small difference ($\varepsilon_V \approx 5\%$) when the flow is attached (upstream of the mast) but large differences are found when the flow is detached (over the camera and wakes of the mast and nuclear load MMRTG). Differences above 40% are found in the wakes of the vision camera and MMRTG. When the flow is detached, no measurements could be done by the rover wind sensor, and therefore the comparison is important in the attached region. Differences on the order of 5% are acceptable. However, for a flow incidence β=180º, the wake of the MMRTG affects slightly the velocity upstream the mast, and results show differences up to 13%, as observed in Fig. 11,which are still acceptable thought more effort could be done to improve these results.

Published by the American Institute of Aeronautics and Astronautics, Inc., with permission. Complete Citation: Bardera, R., Sor, S., Garcia-Magarino, A., Gomez-Elvira, J., Marin, M., Navarro, S., ... & Carretero, S. (2018). Experimental and numerical characterization of the flow around the Mars 2020 rover. Journal of Spacecraft and Rockets, 55(5), 1136-1143. https://doi.org/10.2514/1.A34217

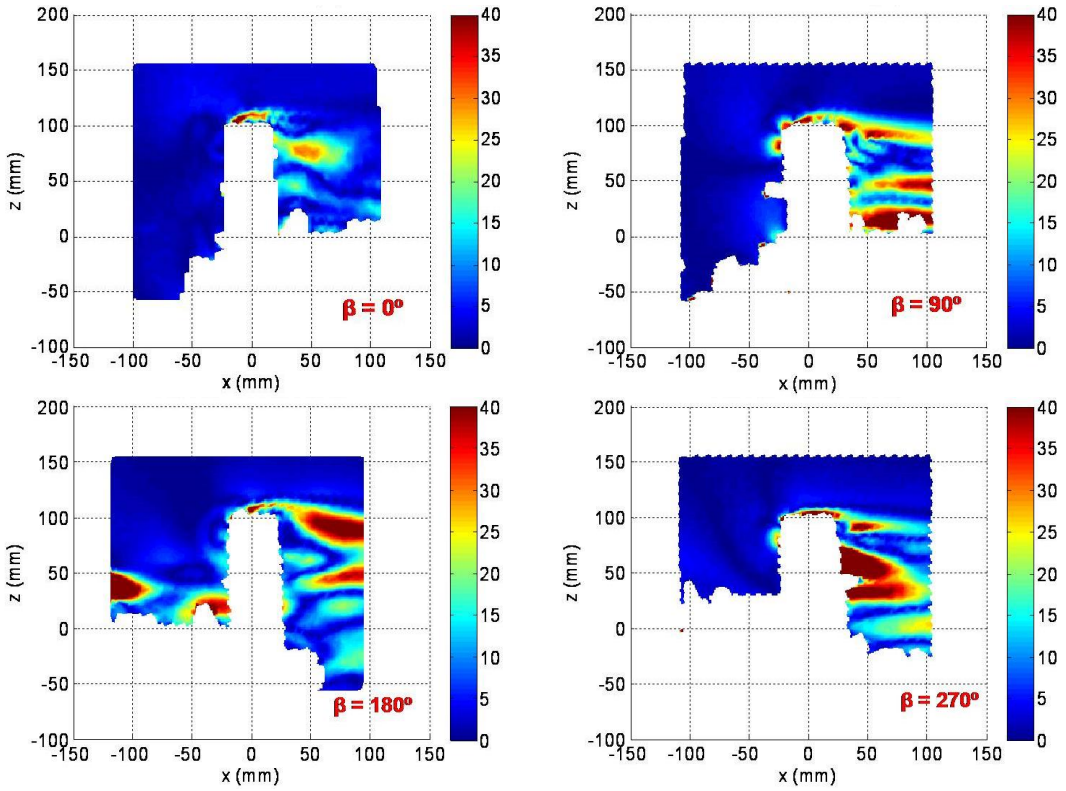

Figure 11. Velocity magnitude differences.

C. Flow angularity differences

Figure 12 shows differences in angular direction of the flow evaluated as an error in pitch angle flow ε_α defined by the following expression,

$$\varepsilon_\alpha = \alpha_{CFD} - \alpha_{PIV} \qquad (8)$$

where α_{CFD} is the pitch as calculated by numerical simulation (CFD), α_{PIV} is the pitch as experimentally determined by PIV technique. The angularity (pitch) of the flow is indicated by the color scale from 0 to 40º. The flow angularity error is very small ($\varepsilon_\alpha \approx 5$º) when the flow is attached but large when the flow is detached. Locations where the flow angle difference is 40° or higher is represented by the red color and is again located in the wake.

Published by the American Institute of Aeronautics and Astronautics, Inc., with permission. Complete Citation: Bardera, R., Sor, S., Garcia-Magarino, A., Gomez-Elvira, J., Marin, M., Navarro, S., ... & Carretero, S. (2018). Experimental and numerical characterization of the flow around the Mars 2020 rover. Journal of Spacecraft and Rockets, 55(5), 1136-1143. https://doi.org/10.2514/1.A34217

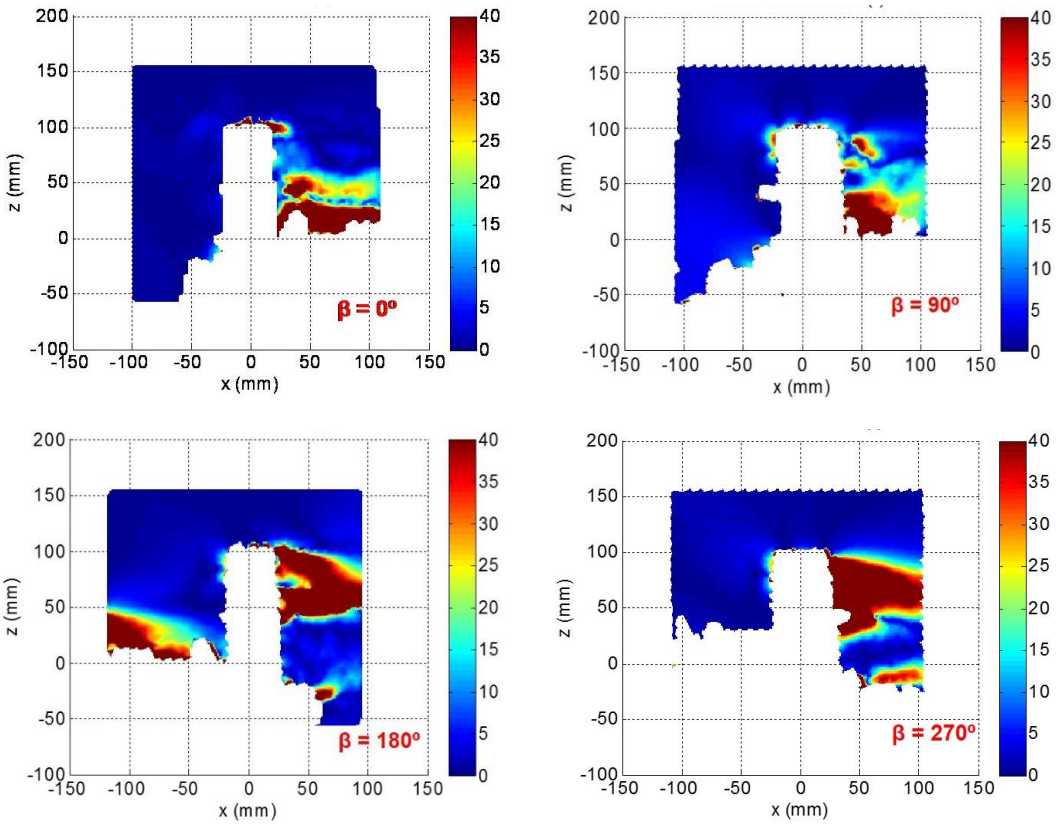

Figure 12. Flow angularity differences.

VII. Conclusions

The flow in the vicinity of the Mars 2020 rover vehicle has been investigated by means of experimental and numerical methods in order to evaluate the flow perturbation produced by the presence of the rover on the Mars Environmental Dynamics Analyzer (MEDA) wind sensors.

The results provide a characterization of the flow field near the Mars 2020 rover, which is placed in a Mars environment, and therefore, provide a deep insight in the environmental interaction of the Mars wind with the rover. The flow structure revealed consisted of two kinds of regions clearly differenciated by upstream and downstream of the mast. The region upstream of the mast is characterized by attached flow with streamlines slightly curved by the presence of the rover vehicle. Downstream of the mast, the flow is separated as typically corresponds to the wake of bluff bodies. The results show that there is indeed an interaction between the Mars wind and the rover, and therefore, a correction of the wind measurements taken by MEDA is needed.

Published by the American Institute of Aeronautics and Astronautics, Inc., with permission. Complete Citation: Bardera, R., Sor, S., Garcia-Magarino, A., Gomez-Elvira, J., Marin, M., Navarro, S., ... & Carretero, S. (2018). Experimental and numerical characterization of the flow around the Mars 2020 rover. Journal of Spacecraft and Rockets, 55(5), 1136-1143. https://doi.org/10.2514/1.A34217

A comparison of results obtained by PIV and CFD was performed in order to evaluate differences between both of them. The results present the advancements in the numerical methods as compared with experimental results in the characterization of the flow field around the Mars 2020 rover. After the analysis of velocity magnitude and angularity of the flow as determined by both methods, experimental and numerical, we can conclude that numerical methods (CFD), in general, are capable to perform a prediction with a minimum error (approx. 5%) of the attached flow but large differences are found when the flow is separated and consequently the sensors booms are located inside the mast wake. At the Reynolds number considered, the effectiveness of numerical methods (CFD) for prediction of the flow upstream of the mast supporting the MEDA wind sensors has been validated by experimental results, providing a reliable method to be used in the future to eliminate the influence of the rover presence on wind data coming from the Mars 2020 rover mission. The results imply an advancement in the space instrumentation carried in the Mars 2020 rover, in particular in the wind sensor. As far as the numerical methods have been proved to be reliable, the correction function for the wind sensor can be obtained in a simple and straightforward method and provide more accurate correction function, resulting in an advancement on the calibration methods in the space instrumentation. However, futher tests are needed to evaluate the numerical methods at different Reynolds numbers.

Aknoledgements

This research has been partially supported by the Spanish Ministry of Economy and Competiveness (MINECO), under project ESP2014-54256-C4-1-R, and also under the Spanish INTA internal Project "Termofluidodinámica".

References

[1]Gómez-Elvira and REMS Team, Environmental Monitoring Instrument for Mars Exploration. Lunar and Planetary Science XXXIX (2008).

[2]Gómez-Elvira, J. et al, REMS: The Environmental Sensor Suite for the Mars Science Laboratory Rover. Space Sci. Rev (2012) 170 pp. 583-640.Springer, 2012.

[3]Domínguez, M., Jiménez, V., Ricart, J., Kowalski, L., Torres, J., Navarro, S., Romeral, J., Castañer, L., A hot film anemometer for the Martian atmosphere. Planetary and Space Science, Vol 56, No. 8, pp:1169-1179. Elsevier, 2008. https://doi.org/10.1016/j.pss.2008.02.013

[4]Chamberlain, T. E., Atmospheric measurements on Mars: the Viking Meteorology Experiment, Bulletin American Meteorological Society, Vol.: 57, No. 9, pp.:1094-1104, Sept. 1976. https://doi.org/10.1175/1520-0477(1976)057<1094:amomtv>2.0.co;2

[5] Hess, S. L., Henry, R. M., Kuettner,J., Leovy, C. B., Ryan, J. A., Meteorology Experiments: The Viking Mars Lander, Icarus, 16, pp. 196 -204 (1972). Academic Press,Inc. 1972. https://doi.org/10.1016/0019-1035(72)90146-7

[6] Seiff, A. et al, The atmosphere structure and meteorology instrument on the Mars Pathfinder Lander, Journal of Geophysical Research, Vol.: 102, No., E2, pp. 4045-4056, Feb. 25, 1997. American Geophysical Union, 1997. https://doi.org/10.1029/96je03320

[7] Greene, G. C. et al, Flow-field measurements around a Mars Lander model using hot-film anemometers under simulated Mars surface conditions. Langley Research Center NASA TN D-6820. NASA Washington DC. Sept. 1972.

[8] Environmental Impact Statement for the Mars 2020 Mission. NASA. Washington DC, 20546. June (2014).

[9] Bhandari, P., Anderson K., CFD Analysis for assessing the effect of wind on the thermal control of the Mars Science Laboratory Curiosity Rover. International Conference on Environmental Systems (ICES). AIAA, 2013, Vail, CO. https://doi.org/10.2514/6.2013-3325

[10] Petrosyan, A. et al, The Martian Atmospheric Boundary Layer, Reviews of Geophysics, 49, RG-3005/2011. American Geophysics Union.

[11] Leovy, C. B., Martian Meteorology, Ann. Rev. Astron. Astrophys. 1979, 17: 387-413. Annual reviews Inc. 1979. https://doi.org/10.1146/annurev.aa.17.090179.002131

[12] White, F., Viscous Fluid Flow, Second Edition, McGraw-Hill, Inc. 1991.

[13]Barlow, J. B., Rae, W. H. Jr.; Pope, A. Low-Speed Wind Tunnel Testing. 3rd Ed.; John Wiley & Sons, Inc. USA 1999.

[14]Raffel, M.,Willert, C. E., Wereley, S. T.,Kompenhans, J., Particle Image Velocimetry: A Practical Guide. Springer, 2007.

[15]Kompenhans, J.,Raffel, M.,Willert, M. PIV Applied to Aerodynamic Investigations in Wind Tunnels. Von Karman Institute for Fluid Dynamics 1996, Lectures Series 1996-03, Rhode Saint Genese, Belgium.

[16]Adrian, R. J.,Westerweel, J. Particle Image Velocimetry, Cambridge University Press, 2011.

[17]Echols, W. H.,Young, Y. A. Studies of portable air-operated aerosol generator. NRL Report 5929, Naval Research Laboratory, Washington, D. C., 1963.

[18] Kähler, C. J.,Sammler, B.,Kompenhans, J. Generation and control of tracer particles for optical flow investigation in air. Experiments in Fluids 2002, 33, 736-742. https://doi.org/10.1007/s00348-002-0492-x

[19] Prasad, A. K. Particle Image Velocimetry. Current Science, Vol. 79, no. 1, 10, 2000.

Published by the American Institute of Aeronautics and Astronautics, Inc., with permission. Complete Citation: Bardera, R., Sor, S., Garcia-Magarino, A., Gomez-Elvira, J., Marin, M., Navarro, S., ... & Carretero, S. (2018). Experimental and numerical characterization of the flow around the Mars 2020 rover. Journal of Spacecraft and Rockets, 55(5), 1136-1143. https://doi.org/10.2514/1.A34217

[20] Lorenz R.D, Sotzen, K.S. Buoyant thermal plumes from planetary landers and rovers: Application to sizing of meteorological masts. Planetary and Space Science 90, pp. 81-89, 2014. https://doi.org/10.1016/j.pss.2013.10.011